J. Phys. B: At. Mol. Phys. 19 (1986) 2715 -2734. Printed in Great Britain

Elastic scattering of electrons by water molecules over the range 100–1000 eV

Akira Katase, Kenji Ishibashi, Yuzuru Matsumoto, Takeji Sakae, Shinya Maezono, Eiji Murakami, Keigo Watanabe and Hideaki Maki

Department of Nuclear Engineering, Kyushu University, Fukuoka, 812 Japan

Received 27 September 1985

Abstract. Relative values of differential cross sections (DCS) are measured by the crossed-beam method. Two cylindrical-mirror energy analysers are employed. One of them is moved to detect scattered electrons at every angle, and the other is fixed at an angle to monitor the elastic scattering events. The effects of target gas distributions in a molecular beam flowing out from a multicapillary array are taken account of to correct the relative values. The DCS are also measured at an angle for water molecules and helium atoms by using a gas chamber. On the basis of the absolute DCS for He measured by Jansen *et al*, the relative DCS for water molecules are converted into absolute values.

In addition, the DCS are calculated by the partial-wave method for the double Yukawa potential. The values of its three adjustable parameters are determined by comparison with the experimental DCS. A spherically symmetric realistic potential is also inferred without adjustable parameters from the charge distribution that was derived from molecular-orbital theory. The DCS calculated for this potential reproduce the experimental values fairly well.

1. Introduction

Interactions of electrons with water molecules are popular and important phenomena in nature. Any nuclear radiation that penetrates into the human body produces therein secondary electrons with appreciable kinetic energy. The water content of the body is about 60% by weight. Interactions of electrons with water are a dominant process among the phenomena induced by nuclear radiation. They cause a biological effect in the human body. Many investigations have been made on the slowing down and energy deposition of electrons in water (Paretzke and Berger 1978, Ritchie *et al* 1978, Hamm *et al* 1980, Turner *et al* 1982, 1983, LaVerne and Mozumder 1983). They have used cross sections for elastic scattering of electrons in water estimated using the Born approximation, because to date few measurements (Trajmar *et al* 1973, Lassettre and White 1973, Bromberg (cited in Lassettre and White), Nishimura 1985) have been carried out on the elastic scattering of electrons by water molecules. It is considered to be useful to obtain the cross sections for water molecules experimentally, even if there are differences in the values of the cross sections between the gaseous and liquid phases (Turner *et al* 1982).

The differential cross sections (DCS) have been calculated for elastic scattering of electrons by water molecules in the Glauber approximation by Fujita *et al* (1983). The results agree with the experimental values only at forward angles and promptly become smaller than those as the scattering angle increases. For the elastic scattering of electrons by rare-gas atoms, the experimental DCS are well reproduced by the DCS

0022-3700/86/172715+20$02.50

calculated using the partial-wave method for the double Yukawa potential with appropriate values of parameters (Green *et al* 1980, 1981). However, the structure of the water molecule is not spherically symmetric and neither is its potential. However, a water molecule has most of its positive charge at its centre. Since this central charge dominates the electric field, the potential is simulated to a good approximation by a potential like that for an atom. Furthermore, the double Yukawa potential may be used as a practical one to give approximate values of DCS. It is interesting to see how the DCS for water molecules calculated using a spherically symmetric potential agree with the experimental DCS and to see the usefulness of the double Yukawa potential for water molecules.

In addition, wavefunctions have been obtained for the ground state of the water molecule by utilising the self-consistent-field molecular-orbital method in the linear combination of atomic orbitals (LCAO) approximation (Ellison and Shull 1955). Banyard and March (1957) have expanded the charge density derived from the above wavefunctions in spherical harmonics and have determined the electron charge distribution averaged over angles $\rho_{00}(r)$. Scattering factors of x-rays calculated from this distribution were shown to agree with the experimental results of Thomer (1937). The scattering factors did not change appreciably by including the second term of the charge density expansion. A static Coulomb potential can be deduced from the distribution $\rho_{00}(r)$ in a spherically symmetric potential approximation. If the DCS calculated from this potential reproduce the experimental values reasonably well, a realistic potential will have been inferred in the approximation of spherical symmetry of the charge distribution in molecules. This may be estimated by the molecular-orbital theory for electrons in molecules. The above comparison will give some insight into the relationship between the structure of a molecule and the scattering phenomena of electrons.

In this work, we present experimental and theoretical studies of the elastic scattering of electrons by water molecules.

2. Experimental apparatus

2.1. Apparatus for the crossed-beam method

For the measurements of the relative DCS, the crossed-beam method was used. A vacuum chamber 64 cm in diameter and 50 cm high was evacuated by two oil diffusion pumps of $1200\,l\,s^{-1}$ and $600\,l\,s^{-1}$ with water baffles and liquid-nitrogen traps. The pressure in the chamber was about 9×10^{-4} Pa during the measurements of cross sections. Three pairs of Helmholtz coils of about 150 cm diameter decreased the residual magnetic field to less than 2 mG in an interaction region of about 10 cm diameter. Two turntables were mounted coaxially in the chamber and could rotate around a vertical shaft of 76 mm diameter. They were driven by stepping motors controlled by a microcomputer. The angle of rotation was read with a protractor graduated on the circumference of each turntable within an accuracy of 0.1°. The central part of the shaft was machined to form a cavity of 60 mm diameter and was used as a vacuum duct for the $600\,l\,s^{-1}$ diffusion pump. A multicapillary array (MCA), through which water molecules flowed out forming a molecular beam, was fitted on the upper end of the shaft so that the centre was on the axis of the shaft. The inner diameter of a capillary of the MCA was 12 μm and the diameter of the MCA was about 1 mm.

An electron gun with a hairpin type tungsten filament (0.15 mm diameter) had four electrodes to focus an electron beam. Its endplate supporting the filament had a hole of 1 mm diameter on the centre axis of the gun. This hole was observed through the exit slit (1 mm diameter) of the focusing electrode using a telescope, for the alignment of the gun. This optical axis or the axis of the gun was adjusted to pass through a definite position above the centre of the MCA, where the electron beam crossed the molecular beam at right angles.

A Faraday cup was mounted on the wall of the vacuum chamber to measure the electron current from the electron gun. The cup was electrically shielded by a grounded metal tube and could be set at any position between the MCA and the chamber wall on the line of the electron beam. The beam current was about 0.5 nA for measurements at forward scattering angles ($\theta \leqslant 30°$) and several nanoamperes at larger angles. The diameter of the electron beam was about 1 mm at the beam crossing point. The width of electron energy distributions was measured to be about 0.7 eV.

A beam of water molecules was introduced into the chamber through the MCA. Distributions of the molecular beam were measured at some positions above the MCA (Sakae *et al* 1986). The halfwidth of the distribution was about 3 mm at a position 2.9 mm above the MCA, where the electron beam crossed the molecular beam. Relative values of DCS were corrected by taking into account this distribution as explained in a later section.

Electrons scattered by water molecules were detected by a channeltron electron multiplier (Ceratron) after energy analysis. A cylindrical-mirror analyser (CMA) was used for this purpose. The radii of the inner and outer electrodes of the CMA were 30 and 75 mm, respectively. The entrance angle of electrons to the CMA was 42.3°. Its entrance slit was a hole of 1.5 mm diameter and its exit slit was a rectangle of 0.5 mm × 5 mm of molybdenum plate. The electron multiplier was biased by a voltage corresponding to about half the electron energy against the exit slit in order to reduce the background count. The energy resolution of the CMA (FWHM) was about 0.6%. The other CMA (M-CMA) was used to monitor the reaction events. This M-CMA was of the same size as the CMA described above and had a slit of larger diameter. The CMA and M-CMA were fixed on the two turntables.

2.2. Gas chamber

The crossed-beam method was used to measure the relative DCS at each incident electron energy. The detection efficiency of the electron multiplier and the transmittance of the CMA may vary with the detected electron energy. Furthermore, the distribution of electron density in the electron beam at the crossing point may depend on the focusing conditions, which should be varied for different electron energies. From these effects, it is difficult to determine the precise relative values of the cross sections for different electron energies by the crossed-beam method. A gas chamber was used in order to obtain the above values at a definite angle of 28°. This chamber was also used for measurements to normalise the relative DCS for water molecules to the absolute DCS for helium.

A cross section through the gas chamber is shown in figure 1. The collimated electron beam passed through a hole of 0.5 mm diameter in an outer sleeve of the gas chamber and entered through a hole of 1 mm diameter into the target gas cell. Its pressure was measured with an MKS Baratron and was controlled automatically by a variable leak valve. The diameters of the two exit holes were 2 mm to ensure that

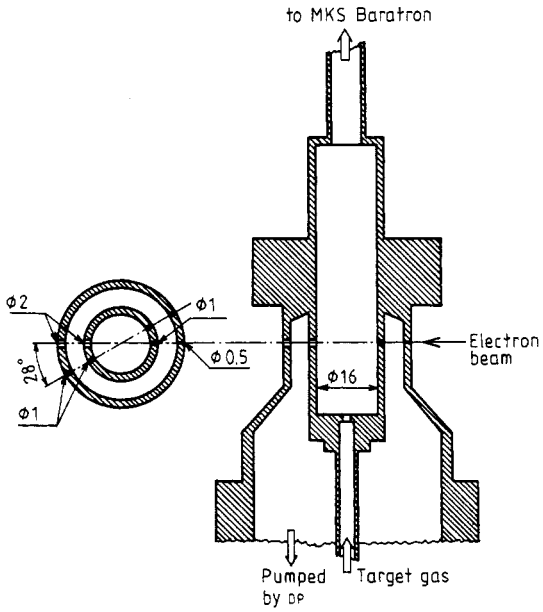

Figure 1. Cross section through the gas chamber.

the outgoing electron beam could leave the cell without colliding against the edges of the holes.

There were additional holes of 1 mm diameter in the inner and outer sleeves at an angle of 28° to the electron beam. The electrons scattered in the gas cell went out through these holes to the CMA for energy analysis. The gas chamber was fixed on the top of the shaft of turntables interchanged with the MCA. The space between the inner and outer sleeves was evacuated by the 600 l s^{-1} diffusion pump. The gas pressure in the gas cell was usually about 0.9 Pa during the measurements.

The vacuum chamber and most of the apparatus were made of 310 or 316L stainless steel.

3. Experimental procedure

3.1. Relative differential cross sections

The crossed-beam method was used for the measurement of the relative DCS for a fixed incident electron energy using the CMA and M-CMA. The number of incident electrons that traverse unit cross section per unit time at position $\boldsymbol{r}$ in the interaction region is defined as $i(\boldsymbol{r})$ (electrons/cm^2 s). The density of the target molecules is specified as $n(\boldsymbol{r})$ (molecules/cm^3) at position $\boldsymbol{r}$. The entrance slit of the CMA (or M-CMA) subtends a solid angle $d\Omega'(\boldsymbol{r})$ to position $\boldsymbol{r}$. If the differential cross section is $d\sigma(\theta')/d\Omega$ for a scattering angle θ', the count rate of the scattered electrons $C_s(\theta)$ is given for the geometrical scattering angle θ by

$$C_s(\theta) = F(\theta) \int \frac{d\sigma(\theta')}{d\Omega} i(\boldsymbol{r}) n(\boldsymbol{r}) \, d\Omega'(\boldsymbol{r}) \, dv \tag{1}$$

where $F(\theta)$ is the detection efficiency of the CMA (or M-CMA) for electrons and dv a small volume element at $\boldsymbol{r}$. The efficiency $F(\theta)$ corresponds to the product of the acceptance of the entrance slit system, the transmittance of the CMA and the detection efficiency of the electron detector. The value of $F(\theta)$ is independent of scattering angle. The above integration is carried out over the interaction region that is accepted by the entrance slit system. The angle θ is determined from the geometrical arrangement of the electron beam and the centres of the MCA and the entrance slit of the CMA (or M-CMA). The variations of $d\sigma(\theta')/d\Omega$ and $d\Omega'(\boldsymbol{r})$ are neglected in the integration, because the dimension of the effective volume in the integration is small compared with the distance between the centre of the MCA and the entrance slit of the CMA. Then

$$C_s(\theta) = F\frac{d\sigma(\theta)}{d\Omega}\Delta\Omega\int i(\boldsymbol{r})n(\boldsymbol{r})\,dv$$

$$= F\frac{d\sigma(\theta)}{d\Omega}\Delta\Omega R(\theta) \tag{2}$$

where

$$R(\theta) = \int i(\boldsymbol{r})n(\boldsymbol{r})\,dv$$

and $\Delta\Omega$ the solid angle of the entrance slit. When the distribution of the molecular beam is narrow, almost all of the interaction region is included in the acceptance angle of the CMA. The value of $R(\theta)$ is then independent of the scattering angle. The value of R, however, may vary depending on the density distributions of electrons in the electron beam and of molecules in the gas beam. If the count rate $C_s(\theta)$ is measured by the CMA for a constant value of R at each angle θ, the results give the relative DCS for fixed incident electron energy. The monitor CMA(M-CMA) is set at a constant angle of 40° to detect the elastically scattered electrons. The number of counts of the M-CMA is proportional to the value of R and is used to monitor the number of events at each scattering angle where the CMA is positioned.

If the distribution of the molecular beam is broad, part of the effective interaction region swells out from the acceptance of the CMA depending on the scattering angle θ. The value of R varies with angle and some correction is necessary to the relative DCS measured. The method of correction will be described in a later section.

The system used for measurements is shown in figure 2. Before a series of measurements was started, the electron beam was scanned around a scattering angle of 0° by the CMA. The distribution of count rates of the CMA as a function of angle gave the profile of the electron beam at the entrance slit of the CMA. Its shape was symmetric in most cases and its peak determined a value on the angular scale that corresponded to zero scattering angle.

The CMA was placed at an angle θ. The counting of CMA and M-CMA signals by a multichannel scaler (MCS) was started simultaneously. When the preset number of counts C_p was detected by the M-CMA, the deflection voltage of the CMA was reduced by 0.1 V and the channel was advanced by one in the MCS. Counts of M-CMA and CMA were then restarted. This process was repeated to obtain the energy spectrum of scattered electrons. The integrated total number of counts of the MCS was denoted as $N_t(\theta)$. The above measurement was carried out at every scattering angle.

The molecular density in the interaction region is composed of two parts: (a) the molecular beam and (b) the background along the electron beam, as shown in figure

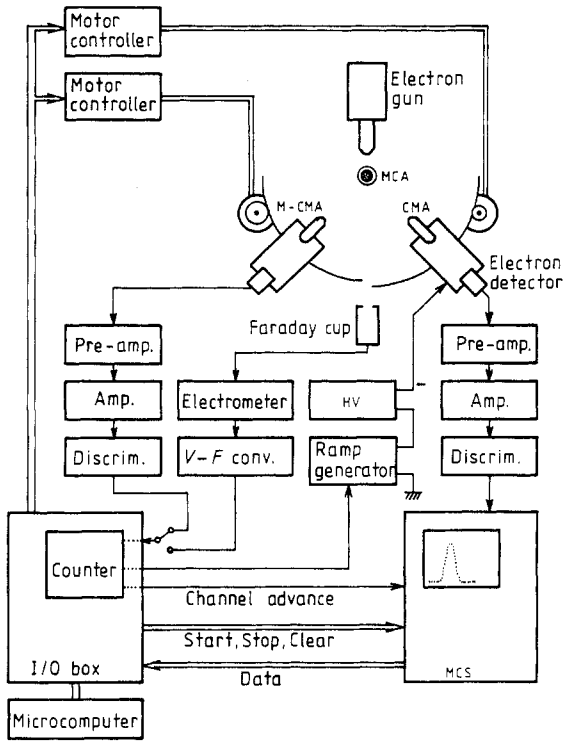

Figure 2. Block diagram of the system for the crossed-beam method to control the measurements and to take data.

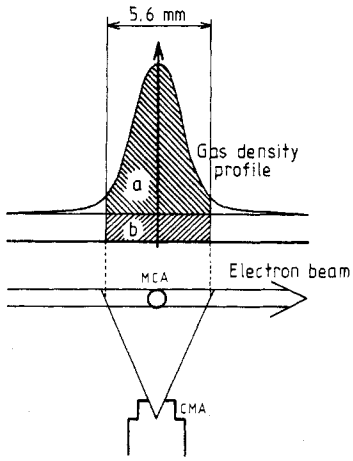

Figure 3. Schematic of density distribution of gas molecules in the interaction region along the electron beam. The part marked 'a' represents the target molecules flowing out from the multicapillary array and part 'b' the background gas molecules.

3. The two vertical lines on both sides of the peak in the figure indicate the acceptance of the CMA for scattered electrons. The contribution of part (b) to $N_t(\theta)$ was estimated experimentally by the following method. The molecular beam from the MCA was stopped and water molecules were introduced into the vacuum chamber from the other port at the same pressure in the chamber as that during the measurements of $N_t(\theta)$. The angular distributions of background counts $N_b(\theta)$ were measured in the same way as that for $N_t(\theta)$, but the preset number of counts C_{pb} was used instead of C_p. In order to relate the values of $N_t(\theta)$ and $N_b(\theta)$ with each other, the electron beam currents were measured with the Faraday cup and were digitised by a voltage-frequency converter. For a constant output from the converter, the numbers of counts N_{tc} and N_{bc} were respectively detected for the gas beam from the MCA and for the background gas at an angle θ_0. If f is defined by the relation

$$f=\frac{N_{bc}}{N_{tc}}\frac{N_t(\theta_0)}{N_b(\theta_0)} \tag{3}$$

the relative DCS are then given by

$$\left(\frac{d\sigma(\theta)}{d\Omega}\right)_R=\sigma_R(\theta)=N_t(\theta)-fN_b(\theta). \tag{4}$$

The value of the ratio N_{bc}/N_{tc} was about 1/15 at an angle of 30°.

In the present measurement, the length of the effective interaction region $l(\theta)$ that is accepted by the CMA is estimated to be 5.6 mm along the electron beam at an angle of 90° from the geometry of the slits of the CMA. This length is not sufficiently large compared with the FWHM value of about 3 mm of the molecular beam profile. Corrections were made to the relative DCS. Relative values of $R(\theta)$ in equation (2) were approximated as being proportional to the molecular density summed along the electron beam in the interaction region accepted by the CMA. This quantity $n_0(\theta)$ was given by the equation

$$n_0(\theta)=\int_{-l(\theta)/2}^{l(\theta)/2} n(r)\,dr \tag{5}$$

where $l(\theta)=5.6/\sin\theta$ in units of millimetres. The measured density distribution (Sakae *et al* 1986) was used as the function $n(r)$. The value of $\sigma_R(\theta)$ obtained above was divided by $n_0(\theta)$ to give the corrected relative DCS. The amount of this correction was about 7% at the maximum.

3.2. Normalisation of differential cross sections between different incident electron energies

The efficiency of the electron detector, the transmittance of the CMA and the value of R may depend on the electron energy. Therefore, the gas chamber was used to measure the relative DCS for different electron energies at a fixed angle of 28°.

At first, helium gas was introduced into the gas cell and during the measurement its pressure was held constant by a pressure controller. Electrons scattered to the CMA were detected at an angle of 28° for a definite amount of integrated beam current for every incident electron energy. The number of counts of the CMA was compared with the values of DCS at 28° which were obtained from the values at 20, 30 and 40° of Jansen *et al* (1976) by using the Lagrange interpolation formula. The ratios of the values of DCS to the number of counts are shown in table 1 normalised to the value for 500 eV. The inverse of these values gives the relative detection efficiency of the CMA system in the present experiment.

Table 1. Normalisation of relative DCS for water molecules to the absolute values.

	E(eV)						
	100	200	300	400	500	700	1000
Ratio	1.36	1.37	1.06	1.04	1.00	1.00	1.06
$\sigma_R(28°)$	3.37	1.96	1.38	1.21	1.00	0.738	0.365
$d\sigma(30°)/d\Omega$ $(10^{-18}\ cm^2\ sr^{-1})$	57.3	32.9	23.2	20.4	17.0	12.5	7.51

Next, water molecules were introduced into the gas cell and the scattered electrons were measured in the same way as for helium for every incident electron energy. The number of counts was multiplied by the values of the ratio obtained above, resulting in the relative DCS, $\sigma_R(28°)$, for different electron energies at the angle 28°. These values normalised to that for 500 eV are also shown in table 1.

3.3 Absolute values of differential cross sections

The present relative DCS were normalised from the following measurements to the absolute values by using the value of 0.111 $a_0^2\,sr^{-1}$ (a_0 is the Bohr radius) for the DCS of helium at 500 eV and 28° evaluated from the data of Jansen *et al* (1976). The gas chamber was used. At the incident electron energy of 500 eV, the numbers of counts of the CMA were measured in the same way as in the above section for several values of the gas pressure in the gas cell for both water molecules and helium atoms. The temperature in the room where the experiments were performed was kept constant to within 0.5° C during the measurements. The results are shown in figure 4. The abscissa shows the gas pressure indicated by the output voltage of the MKS Baratron. The number of counts is proportional to the gas pressure. The ratio of the slopes for the two gases was determined to be 6.61, giving the ratio of the DCS between water molecules and helium atoms at the angle of 28°. Therefore, the DCS for water

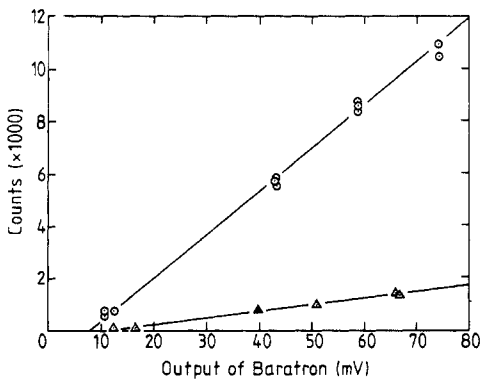

Figure 4. Number of counts of scattered electrons for water molecules (○, 166.1 ± 4.6 counts/mV) and helium atoms (△, 25.1 ± 1.0 counts/mV) as a function of gas pressure in the gas cell, which is shown by the output voltage of the MKS Baratron. The incident electron energy is 500 eV.

molecules

σ_{H_2O} (550 eV, 28°) $= 6.61 \times 0.111\ a_0^2\ sr^{-1} = 0.734\ a_0^2\ sr^{-1} = 20.6 \times 10^{-18}\ cm^2\ sr^{-1}$.

From the values of $\sigma_R(28°)$ in the preceding section, the absolute values of DCS were deduced for other energies at 28°. The ratios $\sigma(30°)/\sigma(28°)$ were estimated from the measured relative DCS at angles 20, 30 and 40° by the same interpolation method as before. The aboslute DCS at 30° then resulted from the ratios $\sigma(30°)/\sigma(28°)$ and the absolute values at 28°. On the basis of these values at 30°, all the relative values were converted into the absolute DCS.

4. Results

The DCS for elastic scattering are listed in table 2 for incident electron energies of 100, 200, 300, 500, 700 and 1000 eV. They are also plotted in figure 5. The errors are mostly due to those in the absolute values used for normalisation. Total cross sections $\sigma(E)$ were evaluated by integrating the DCS. The experimental DCS were fitted by the square of the Legendre polynomials at the forward and backward angles, respectively. Values at 180° were assumed to be those with 10% errors calculated for the double Yukawa potential that will be described later and they were included in the fitting at backward angles. Values of DCS estimated by this method are shown in table 2 within parentheses. Cross sections for momentum transfer $\sigma_M(E)$ were also obtained and are listed in table 2.

5. Calculations of the differential elastic scattering cross sections

The charge distribution of water molecules is governed mainly by the central oxygen atom, but it is not spherically symmetric and has a dipole moment of 1.8 D. While the effect of the dipole moment is significant in scattering of electrons at low incident energy, it may be less important in the present energy range above 100 eV. The Coulomb potential of water molecules is approximated by a spherically symmetric potential $V(r)$. Therefore, the partial-wave method is used to calculate the cross sections.

The Schrödinger equation to be solved is given by

$$[-d^2/dr^2 + U(r) + l(l+1)/r^2]u_l(r) = k^2 u_l(r) \tag{6}$$

where u_l is the partial wave for the orbital angular momentum $l\hbar$, k the wavenumber and $U(r) = 2\mu V(r)/\hbar^2$. Atomic units are used in the following.

5.1. Double Yukawa potential

The double Yukawa potential has been used in calculations of DCS for elastic scattering of electrons by atoms. The calculated results agree well with the experimental DCS after adjustment of the values of the parameters in the potential (Green *et al* 1980, 1981). A potential of this form has been used in the present calculation and is given as

$$U(r) = -2(Z/r)G(r) \tag{7}$$

where $G(r)$ is a screening function:

$$G(r) = (1/H)\, e^{-r/d} + (1 - 1/H)\, e^{-r/s}. \tag{8}$$

The three quantities H, d and s are the adjustable parameters to be determined from the comparison of the calculated and the measured DCS.

Table 2. Differential cross sections for elastic electron scattering by water molecules. Values in parentheses are those estimated by extrapolation. The symbols σ and σ_M are the total elastic and momentum transfer cross sections, respectively. Cross sections are in units of 10^{-16} cm^2 sr^{-1}, and their errors are shown under the cross section in per cent. Total and momentum transfer cross sections are in units of 10^{-16} cm^2.

Angle (deg)	E (eV)						
	100	200	300	400	500	700	1000
0	(9.71)	(12.0)	(8.54)	(8.71)	(6.53)	(5.90)	(4.47)
5	(8.34)	9.70	6.99	6.88	5.23	4.74	3.67
		13	13	12	8	13	13
10	5.44	4.09	3.29	2.91	2.28	1.95	1.25
	12	13	13	12	8	13	13
15	2.96	2.02	1.64	1.27	0.957	0.767	0.500
	12	13	13	12	9	13	13
20	1.59	1.03	0.727	0.597	0.487	0.357	0.246
	12	13	13	12	9	13	13
30	0.573	0.329	0.232	0.204	0.170	0.125	0.0751
	12	12	12	12	8	12	13
40	0.228	0.158	0.114	0.0874	0.0744	0.0524	0.0300
	12	12	13	12	9	13	13
50	0.129	0.0822	0.0595	0.0460	0.0403	0.0260	0.0148
	12	12	13	12	9	13	13
60	0.0785	0.0489	0.0381	0.0308	0.0255	0.0162	0.00872
	12	12	13	12	9	13	13
70	0.0498	0.0326	0.0283	0.0219	0.0163	0.0106	0.00534
	12	12	13	12	9	13	13
80	0.0286	0.0263	0.0218	0.0157	0.0120	0.00724	0.00372
	12	12	13	12	9	13	13
90	0.0251	0.0254	0.0187	0.0128	0.00973	0.00535	0.00267
	12	12	12	12	9	13	13
100	0.0287	0.0245	0.0158	0.0110	0.00831	0.00427	0.00214
	12	12	13	12	9	13	13
110	0.0388	0.0246	0.0151	0.0102	0.00711	0.00353	0.00172
	12	12	13	12	9	13	13
120	0.0531	0.0242	0.0145	0.00953	0.00629	0.00303	0.00148
	12	12	12	12	9	13	13
130	0.0680	0.0245	0.0142	0.00911	0.00607	0.00269	0.00136
	12	12	13	12	9	13	13
140	(0.0984)	(0.0293)	(0.0155)	(0.00915)	(0.00577)	(0.00255)	(0.00130)
150	(0.132)	(0.0356)	(0.0170)	(0.00924)	(0.00571)	(0.00250)	(0.00131)
160	(0.167)	(0.0429)	(0.0186)	(0.00938)	(0.00572)	(0.00251)	(0.00134)
170	(0.192)	(0.0487)	(0.0198)	(0.00949)	(0.00575)	(0.00253)	(0.00137)
180	(0.202)	(0.0510)	(0.0203)	(0.00953)	(0.00576)	(0.00254)	(0.00138)
σ	2.98	2.11	1.56	1.32	1.04	0.819	0.548
	12	12	12	12	9	13	13
σ_M	1.01	0.464	0.296	0.208	0.156	0.0930	0.0515
	12	12	12	12	9	13	13

Phaseshifts are given in the Born approximation for the double Yukawa potential by the equation

$$\delta_{l,B} = \tan^{-1}\left\{\frac{Z}{k}\left[\frac{1}{H}\,Q_l\left(1+\frac{1}{2k^2d^2}\right)+\left(1-\frac{1}{H}\right)Q_l\left(1+\frac{1}{2k^2s^2}\right)\right]\right\} \tag{9}$$

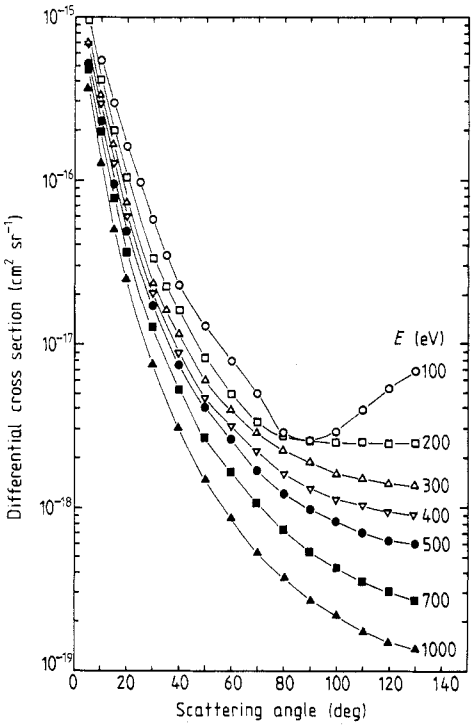

Figure 5. Differential cross sections for elastic electron scattering by water molecules measured for various incident electron energies. Curves are shown connecting experimental points.

where Q_l is the Legendre function of the second kind (Green *et al* 1980). The phaseshift δ_l that was obtained by numerically solving equation (6) was seen to be nearly equal to $\delta_{l,B}$ for l larger than l_{mid}. (The value of l_{mid} is 6–10 depending on the incident electron energy.) In the numerical calculations of δ_l for larger values of l, the step Δr of numerical integration should be made smaller than that for smaller values of l to avoid the accumulation of error in the calculation. This requires a longer calculation time for larger l. Therefore, we used $\delta_{l,B}$ instead of δ_l for $l \geqslant l_{mid}+1$, smoothly connecting $\delta_{l,B}$ to δ_l at $l = l_{mid}$ by multiplying by a factor that was nearly equal to unity.

Before adjusting the values of the three parameters in the potential, comparisons were made between the calculated and measured cross sections by varying the values of just two parameters, d and H. A relation $s = d/(1+H)$ (Green *et al* 1980) was used to obtain the value of s. Agreements were not good. The calculated DCS deviate from the measured results by more than 50% at backward scattering angles. Therefore, the values of the three parameters were adjusted independently, making the calculated DCS agree with the measured ones.

5.2. Realistic potential

The double Yukawa potential described above has been proposed to approximate the potential of an atom that has a positive charge Ze at the origin. An electric charge

distribution $\rho(r)$ is obtained for a potential $V(r)=(\hbar^2/2\mu)U(r)$ in esu by the equation

$$\rho(r)=\frac{1}{4\pi}\nabla^2(-\tfrac{1}{2}U(r))$$

$$=\frac{1}{4\pi}\frac{Z}{r}\frac{\mathrm{d}^2G(r)}{\mathrm{d}r^2}. \tag{10}$$

For the double Yukawa potential of equations (7) and (8), $\rho(r)$ is given by

$$\rho(r)=\frac{1}{4\pi}\frac{Z}{r}\left[\frac{1}{d^2H}\mathrm{e}^{-r/d}+\frac{1}{s^2}\left(1-\frac{1}{H}\right)\mathrm{e}^{-r/s}\right]. \tag{11}$$

On the other hand, an electron charge distribution averaged over angles $\rho_{\mathrm{EB}}(r)$ has been obtained for water molecules in the LCAO approximation (Ellison and Shull 1955, Banyard and March 1957). The spherical charge density $4\pi r^2\rho_{\mathrm{EB}}$ has two maxima at $r=0.1$ and 1.0 a_0, while $4\pi r^2\rho$ has peaks at $r=0.014$ and 0.5 a_0. The latter charge density distribution is much different from the former. From the charge distribution ρ_{EB}, a potential is inferred that will represent the Coulomb potential of water molecules more realistically.

The charge distribution ρ_{EB} is approximated to have an analytic form

$$4\pi r^2\rho_{\mathrm{EB}}(r)=a_2r^2\,\mathrm{e}^{-r/b_2}+a_3r^3\,\mathrm{e}^{-r/b_3} \tag{12}$$

where a_2, b_2, a_3 and b_3 are adjustable parameters and are determined in the following. The shielding function $G_{\mathrm{EB}}(r)$ is deduced by integrating $\rho_{\mathrm{EB}}(r)$ twice, as seen in equation (10). Then

$$G_{\mathrm{EB}}(r)=(1/Z)[a_2b_2^2(r+2b_2)\,\mathrm{e}^{-r/b_2}+a_3b_3^2(r^2+4b_3r+6b_3^2)\,\mathrm{e}^{-r/b_3}]. \tag{13}$$

When the value of r is close to zero, the potential $U_{\mathrm{EB}}(r)$ should be the Coulomb potential and $G_{\mathrm{EB}}(0)=1$. Under this condition, values of the parameters in ρ_{EB} were determined from comparison with the density distribution of Banyard and March (1957) as

$$a_2=4478 \qquad b_2=0.0602$$

$$a_3=125 \qquad b_3=0.322.$$

For the potential $U_{\mathrm{EB}}(r)=-2(Z/r)G_{\mathrm{EB}}(r)$, the phaseshifts are given in the Born approximation by

$$\delta_{l,\mathrm{B}}=\tan^{-1}\left\{\frac{a_2b_2^2}{k}\left[b_2Q_l(x_2)-\left(\frac{1}{2b_2k^2}\right)Q_l'(x_2)\right]\right.$$

$$\left.+\frac{a_3b_3^2}{k}\left[b_3^2Q_l(x_3)-\left(\frac{3}{2k^2}\right)Q_l'(x_3)+\left(\frac{1}{2b_3^2k^4}\right)Q_l''(x_3)\right]\right\} \tag{14}$$

where

$$x_2=1+1/2k^2b_2^2 \qquad x_3=1+1/2k^2b_3^2. \tag{15}$$

Using a value of 10 for Z, the DCS were calculated using the same method as in § 5.1. Their values were larger than the measured DCS by a factor of about 2. These larger values were considered to be due to the presence of the positive charge $10e$ at the origin in contrast to $8e$. Therefore, the potential was modified as follows. The hydrogen nuclei are not at the centre of a water molecule. They are situated at a distance

of r_{OH} ($=1.81\ a_0$) from the oxygen nucleus. Now, the hydrogen nuclei, or protons, are assumed to be distributed spherically and uniformly around the oxygen nucleus in the form of a shell with radius r_{OH}. Therefore, a realistic potential $U_R(r)$ is deduced to be

$$U_R(r) = -(2/r)(10G_{EB} - 2 + 2f_p) \tag{16}$$

where

$$f_p = \begin{cases} r/r_{OH} & \text{for } r \leq r_{OH} \\ 1 & \text{for } r > r_{OH}. \end{cases} \tag{17}$$

For this potential, the magnitude of the charge present at the centre is $+8e$. For $r > r_{OH}$, the potential $U_R(r)$ is equal to $U_{EB} = -2(Z/r)G_{EB}$ with the central charge of $+10e$. For $r < r_{OH}$, the potential $U_R(r)$ is a little larger than that produced for $+8e$. By using this realistic potential U_R, the DCS were calculated. For l larger than l_{mid}, the Born phaseshifts $\delta_{l,B}$ of equation (14) were used. In the calculation, the values of l_{mid} were 5 for incident electron energy 100 eV, 6 for 200 eV and 10 for 300 to 1000 eV.

6. Discussion

6.1. Comparison of the present experimental results with previous experiments

Only a few experiments have been done on electron scattering by water molecules. The DCS have been measured by Lassettre and White (1973) and Bromberg (cited in Lassettre and White) at forward angles for an incident electron energy of 500 eV. Both results are nearly equal. The present work compares very nicely with that of Bromberg, as shown in figure 6. Nishimura (1985) has measured the DCS for incident electron energies of 40 to 200 eV. For scattering of 100 eV electrons, the present results are larger by 8–40% than those of Nishimura over all angles, as shown in figure 7. For scattering of 200 eV electrons, our results agree fairly well with those of Nishimura at backward angles. At forward angles the former are larger by 30–60% than the latter.

As for the total cross sections, our results are compared with those of Nishimura (1985) and Brüche (1929) in figure 8. Our results are larger than those of Nishimura, as expected because of the difference in the DCS. The present values are considered

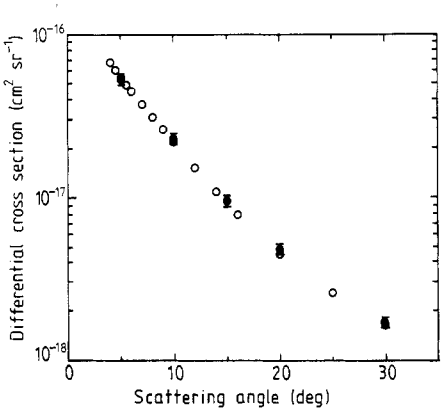

Figure 6. Comparison of the present DCS (●) with those of Bromberg (○). The incident electron energy is 500 eV.

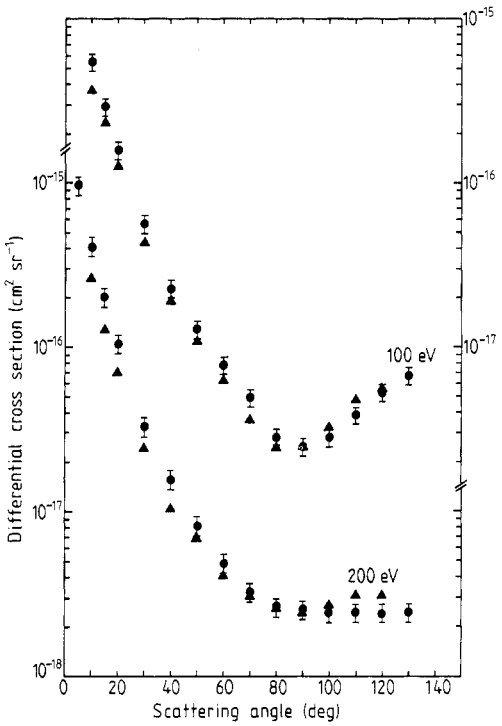

Figure 7. Comparison of the present DCS (●) with those of Nishimura (1985) (▲) for incident electron energies of 100 and 200 eV. (Note that results at 100 eV refer to the right-hand scale.)

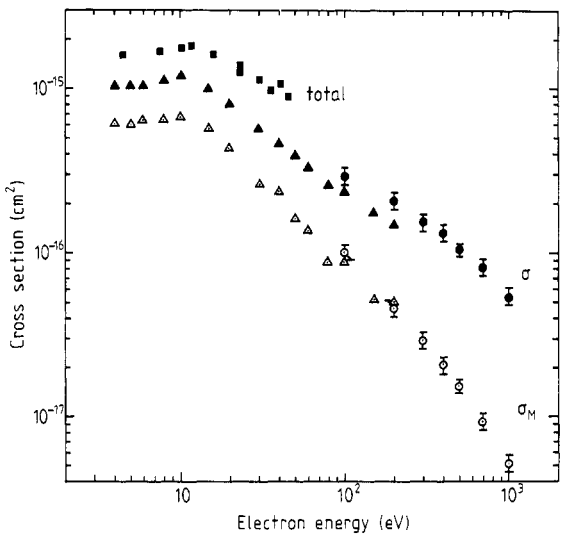

Figure 8. Total scattering cross sections as a function of electron energy. Full squares (■) are the data of Brüche (1929) for total cross sections including cross sections of other reactions in addition to those of elastic scattering. Full and open triangles are for elastic scattering (▲) and momentum transfer (△) cross sections of Nishimura (1985). Full and open circles show cross sections of the present work for elastic scattering (●) and momentum transfer (○).

to be reasonable in comparison with those of Brüche. His results are the total reaction cross sections including the cross sections for other reactions in addition to those for elastic scattering. Cross sections for momentum transfer are also shown in the figure.

6.2. Comparison of measured cross sections with theory

6.2.1. Double Yukawa potential. As described in § 5.1, the double Yukawa potential with three adjustable parameters was used to calculate the DCS by the partial-wave method. The values of the three parameters were determined by the least-squares method for an incident electron energy of 1000 eV from comparison of the calculated DCS with the experimental values. The results are $H = 1.4714$, $d = 0.5287$ and $s = 0.0141$. The DCS for other incident electron energies were calculated using these values of the parameters. The calculated values of phaseshifts are shown in figure 9 and the DCS calculated are shown in figure 10 along with the experimental results. The calculated values reproduce well the measured DCS for all incident electron energies and scattering angles except at forward angles for low incident energies. The spherically symmetric potential can be used as a substitute for the real potential of water molecules for elastic electron scattering in the present energy range.

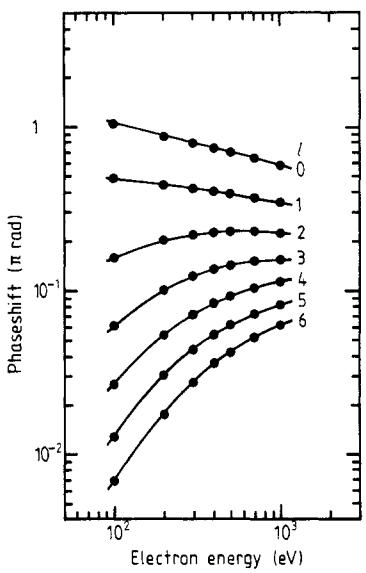

Figure 9. Phaseshifts for the partial waves with $l = 0$ to 6 for scattering by the double Yukawa potential, as a function of incident electron energy. Parameter values: $H = 1.471$, $d = 0.5287$, $s = 0.0141$.

In the present double Yukawa potential, the value of s is considerably smaller than that of d. Therefore, the potential is approximated by a single Yukawa potential or a screened Coulomb potential with a central charge of $ZH = 6.8$. The DCS calculated for this potential deviate from those for the double Yukawa potential by about 10% only for backward angles. The potential for water molecules is approximated tolerably well by a screened Coulomb potential with an appropriate central charge in some cases.

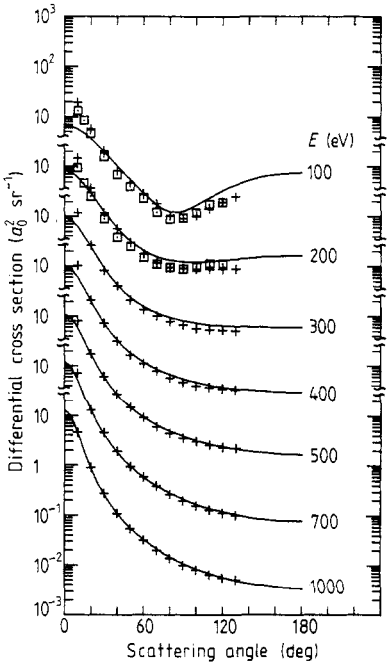

Figure 10. Differential cross sections calculated for the double Yukawa potential. The values of the three parameters in the potential are as shown in figure 9. Curves are the calculated DCS. Crosses (+) are the experimental DCS of the present work. Results of Nishimura (1985) are represented by open squares (□). (Note displacement of vertical scale.)

6.2.2. Differential cross sections in the Born approximation. The DCS were also calculated as a function of the momentum transfer q in the Born approximation with the above values of the parameters using the scattering amplitude (Green *et al* 1980) given by

$$f_B(q) = 2Z[H^{-1}/(q^2+d^{-2})+(1-H^{-1})/(q^2+s^{-2})]. \tag{18}$$

The results are shown in figure 11(a) along with the experimental results. The experimental values are already seen to deviate slightly from the curve for an incident energy of 1000 eV. However, for higher energies, the DCS calculated in the Born approximation are expected to give good values for elastic scattering cross sections using the scattering amplitude of equation (18) with the present parameter values.

Small-angle scattering of high-energy electrons has been measured for water molecules by Konaka (1972) and Shibata *et al* (1980) for 42 and 30 keV electrons, respectively. Their results are compared in figure 11(b) with the present curve computed in the Born approximation, which is the same as that in figure 11(a). The above two experimental results were normalised to the curve at momentum transfer q of about 2.0 in atomic units, because the absolute values were not given. Representative values were read from the figure of Shibata *et al*, showing the experimental data for elastic scattering. These results agree well with the present curve. The results of Konaka are for total scattering. In the experimental results of Shibata *et al* the intensity for total scattering varies nearly proportionally to that for elastic scattering for momentum

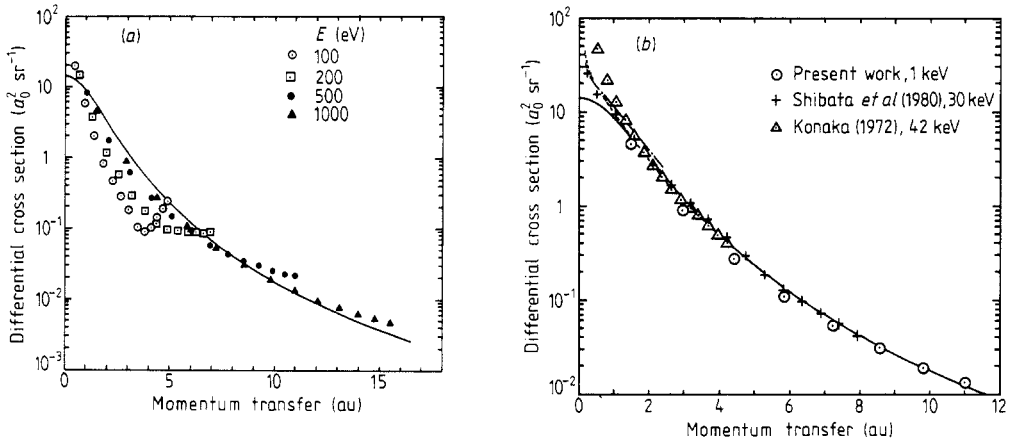

Figure 11. Differential cross sections calculated in the Born approximation for the double Yukawa potential with the present parameter values (as in figure 9). The DCS from the Born approximation are shown as a full curve (——). (*a*) Comparisons with the present experimental results. (*b*) Comparisons with the data obtained from the scattering of high-energy electrons. They are normalised to the curve at a momentum transfer of about 2.0. Other theoretical results are shown by a chain curve (— · —) (Sharma and Tripathi 1983) and a broken curve (- - -) (Szabo and Ostlund 1974).

transfer q larger than about 2. The values given by Konaka show the same variation with momentum transfer as that of the curve for the above region.

The DCS have been calculated by Szabo and Ostlund (1974) for a momentum transfer of 0.1–2.6 with CNDO wavefunctions. They are shown as a broken curve in figure 11(*b*). The theoretical values agree with the present curve for momentum transfer above about 1.0. The DCS have also been calculated by Sharma and Tripathi (1983). Their values are greater than those of Szabo and Ostlund by about 10% for momentum transfer larger than 0.5 and, therefore, they deviate upwards from the present curve. For a complete check of the present DCS obtained in the Born approximation, the absolute DCS need to be measured for the scattering of high-energy electrons.

6.2.3. Realistic potential. The charge distribution producing the present double Yukawa potential is appreciably different from that estimated by the molecular-orbital theory, as shown in figure 12. In spite of this difference, the measured DCS were well reproduced by the calculation using this potential with the appropriate values of parameters. From the charge distributions estimated from the wavefunctions for water molecules, the realistic potential was inferred as described in § 5.2. This potential has no adjustable parameters. The DCS calculated are shown as curves in figure 13 along with the experimental results, indicating the good agreement between them in shape and absolute value except at forward angles less than 20° for the low incident electron energies. The calculated values are slightly larger than the measured DCS at backward angles. For the incident electron energy of 100 eV, deviations of the calculated DCS from the measured results are also seen at about 90°. The details of the charge distribution or its deviations from spherical symmetry are considered to increase their effect on the elastic scattering for lower incident energy.

The double Yukawa potential is compared with the realistic potential in figure 14. The two potentials have nearly equal values near the origin ($r < 0.5$) and decrease in

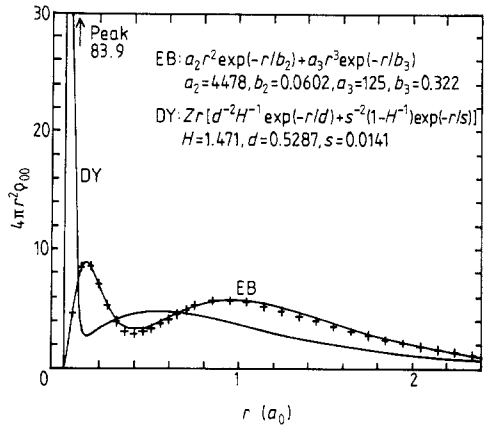

Figure 12. Electron charge distributions in water molecules. The curve DY shows the distribution for the double Yukawa potential. Values of parameters in the potential are shown. The curve EB is a distribution given in the work of Banyard and March (1957). Crosses are the values computed from equation (12) with the present parameter values.

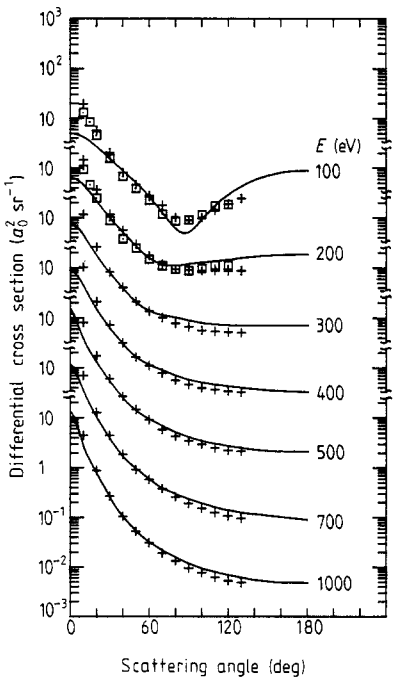

Figure 13. Differential cross sections calculated for the realistic potential (full curves). Crosses (+) are the experimental DCS of the present work. Squares (□) are from Nishimura (1985). (Note displacement of vertical scale.)

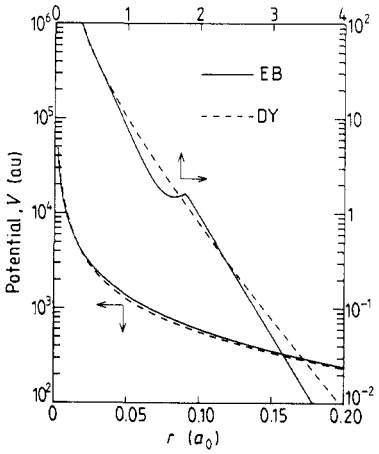

Figure 14. Spherically symmetric potentials $V(r)$ for water molecules as a function of the distance from the centre. The full curve is for the realistic potential given by equation (16) and the broken curve for the double Yukawa potential with the present parameter values.

a fairly similar manner up to a distance of 3 au. As seen in figure 12, there is a sharp peak near the origin in the electron density distribution for the double Yukawa potential. This peak compensates the positive charge, resulting in a reasonable amount of positive charge near the origin. There is a difference between the two potentials around $r = 1.8$ au because of the presence of the proton shell. The agreement of the DCS calculated for these potentials shows that the differences between them for larger values of r do not affect the scattering phenomena appreciably and that the disparity around 1.8 au is considered to be averaged to give the analogous effect.

7. Conclusions

Absolute values of the DCS have been obtained, normalised to those for helium by Jansen *et al* (1976) for 500 eV incident electron energy. The present values agree very well with the available data of Bromberg. The present relative values of the DCS are considered to be much more reliable for each of the incident electron energies, because the elastic events were always monitored by one of the electron detectors during the measurements of the angular distributions.

The double Yukawa potential was used to compute the DCS. The values of three adjustable parameters in the potential were determined from the DCS measured for 1000 eV incident electron energy. The calculated DCS satisfactorily reproduced the experimental results for other incident energies. For incident energies above 1000 eV, the correct values of the DCS are expected to be derived in the Born approximation with the present parameter values.

The realistic potential was inferred without adjustable parameters from the electron and proton charge distributions in water molecules, which were assumed to be spherically symmetric. The DCS calculated by using this potential showed fairly good agreement with the experimental results in shape and absolute value.

Acknowledgments

The authors thank K Oheda and T Kinoshita for their contributions to the preliminary experiments of this study. We are grateful to T Hama and T Shibata for the construction of the apparatus.

References

Banyard K E and March N H 1957 *J. Chem. Phys.* **26** 1416-20
Brüche E 1929 *Ann. Phys., Lpz.* **1** 93-134
Ellison F O and Shull H 1955 *J. Chem. Phys.* **23** 2348-57
Fujita T, Ogura K and Watanabe Y 1983 *J. Phys. Soc. Japan* **52** 811-7
Green A E S, Rio D E and Ueda T 1981 *Phys. Rev.* A **24** 3010-8
Green A E S, Schippnick P F, Rio D E and Ganas P S 1980 *Int. J. Quantum Chem., Quantum Chem. Symp.* **14** 71-82
Hamm R N, Turner J E, Wright H A and Ritchie R H 1980 *Seventh Symposium on Microdosimetry* vol I pp 717-26
Jansen R H J, de Heer F J, Luyken H J, van Wingerden B and Blaauw H J 1976 *J. Phys B: At. Mol. Phys.* **9** 185-212
Konaka S 1972 *Japan J. Appl. Phys.* **11** 1199-204
Lassettre E N and White E R 1973 *J. Chem. Phys.* **60** 2460-9
LaVerne J A and Mozumder A 1983 *Radiat. Res.* **96** 219-34
Nishimura H 1985 private communication; *J. Phys. Soc. Japan* **54** 1224-7
Paretzke H G and Berger M J 1978 *Sixth Symposium on Microdosimetry* vol I pp 749-58
Ritchie R H, Hamm R N, Turner J E and Wright H A 1978 *Sixth Symposium on Microdosimetry* vol I pp 345-54
Sakae T *et al* 1986 to be published
Sharma B S and Tripathi A N 1983 *J. Phys. B: At. Mol. Phys.* **16** 1827-35
Shibata S, Hirota N, Kakuta N and Muramatsu T 1980 *Int. J. Quantum Chem.* **18** 281-5
Szabo A and Ostlund N S 1974 *J. Chem. Phys.* **60** 946-50
Thomer G 1937 *Phys. Z.* **38** 48-57
Trajmar S, Williams W and Kuppermann A 1973 *J. Chem. Phys.* **58** 2521-31
Turner J E, Magee J L, Wright H A, Chattergee A, Hamm R N and Ritchie R H 1983 *Radiat. Res.* **96** 437-49
Turner J E, Paretzke H G, Hamm R N, Wright H A and Ritchie R H 1982 *Radiat. Res.* **92** 47-60